Environmental Science & Technology

pubs.acs.org/est

Article

Anaerobic Dissolution Rates of U(IV)-Oxide by Abiotic and Nitrate-Dependent Bacterial Pathways

Maria P. Asta,* Harry R. Beller, and Peggy A. O'Day

Cite This: *Environ. Sci. Technol.* 2020, 54, 8010–8021

Read Online

ACCESS | Metrics & More | Article Recommendations | Supporting Information

ABSTRACT: The long-term stability of U(IV) solid phases in anaerobic aquifers depends upon their reactivity in the presence of oxidizing chemical species and microbial catalysts. We performed flow-through column experiments under anaerobic conditions to investigate the mechanisms and dissolution rates of biogenic, noncrystalline $UO_2(s)$ by chemical oxidants (nitrate and/or nitrite) or by *Thiobacillus denitrificans*, a widespread, denitrifying, chemolithoautotrophic model bacterium. Dissolution rates of $UO_2(s)$ with dissolved nitrite were approximately 5 to 10 times greater than with nitrate alone. In the presence of wild-type *T. denitrificans* and nitrate, $UO_2(s)$ dissolution rates were similar to those of abiotic experiments with nitrite (from 1.15×10^{-14} to 4.94×10^{-13} mol m^{-2} s^{-1}). Experiments with a *T. dentrificans* mutant strain defective in U(IV) oxidation supported microbially mediated U(IV) oxidation. X-ray absorption spectroscopy (XAS) analysis of post-reaction solids showed the presence of mononuclear U(VI) species rather than a solid U(VI) phase. At steady-state U release, kinetic and spectroscopic results suggest detachment of oxidized U(VI) from the $UO_2(s)$ surface as the rate-determining step rather than electron transfer or ion diffusion. Under anaerobic conditions, production of nitrite by nitrate-reducing microorganisms and enzymatically catalyzed, nitrate-dependent U(IV) oxidation are likely dual processes by which reduced U solids may be oxidized and mobilized in the aqueous phase.

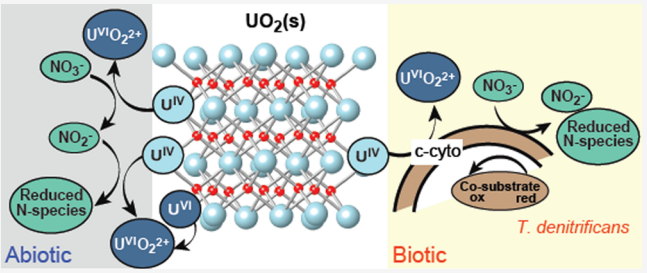

INTRODUCTION

Uranium (U) groundwater contamination is a worldwide environmental concern. Stimulated in situ bioreduction of dissolved U(VI) and precipitation as a poorly soluble U(IV) oxide (nominally $UO_2(s)$) has received considerable attention as a remediation approach for immobilizing U in aquifers under moderately reducing conditions (known as reductive immobilization).[1−5] Nanoparticulate uraninite ($UO_{2+x}(s)$)[6,7] and noncrystalline disordered U(IV) (monomeric and polymeric U(IV)-oxides)[8−10] have been reported as the products of microbially reduced U(VI). The presence of multiple U(IV) species has been reported in field sediments[5,11−13] and laboratory experiments.[14] Some of these studies proposed that uraninite was the end product of abiotic reduction of U(VI),[5,12] which, in complex systems such as natural sediments, may occur concomitantly with biological U(VI) reduction,[12] whereas others suggested precipitation of noncrystalline U(IV) species and transformation to nanocrystalline uraninite with aging.[14,15] Microbially mediated U(IV) oxidation under anaerobic conditions may remobilize these U(IV) forms and thus render long-term reductive immobilization less effective.[16−21] Therefore, identifying mechanisms and quantifying rates of U release from reoxidation and dissolution of $UO_2(s)$ and related U(IV) solid-phase contaminants are important for understanding potential U mobility in the environment.

Abiotic oxidation of $UO_2(s)$ by molecular O_2 proceeds rapidly and oxidation rates have been investigated under a variety of conditions, including variable pO_2, pH, and dissolved inorganic carbon and cations.[22,23] Dissolution rates of $UO_2(s)$ produced by microbial reduction (biogenic $UO_{2+x}(s)$) under anaerobic and aerobic conditions were found to be within experimental error of those of chemically synthesized $UO_2(s)$ in carbonate-free systems in one study.[22] Another study proposed that chemogenic uraninite was more resistant to oxidation than forms of biogenic U(IV)-oxides in the presence of dissolved oxygen.[23] Monomeric forms of U(IV) have been found to be less stable and more susceptible to oxidation than biogenic uraninite under anoxic condtions.[22] However, Cerrato et al.[23] suggested that exposure of biogenic U(IV) solids to oxidants and transport processes that control exposure and U release are more important than the actual form of the solid, given relatively small differences observed in the oxidation rate constants of biogenic uraninite and monomeric U(IV) in the presence of oxygen.

Received: February 18, 2020
Revised: May 29, 2020
Accepted: May 29, 2020
Published: May 29, 2020

https://dx.doi.org/10.1021/acs.est.0c01019
Environ. Sci. Technol. 2020, 54, 8010–8021

Anaerobic oxidation of U(IV) solids in the presence of dissolved nitrate (NO_3^-) and its reduction products is of particular concern in subsurface U.S. Department of Energy sites and other sites worldwide where U and nitrate are found as co-contaminants.[17,24−30] In anaerobic systems, the abiotic oxidation of UO_2(s) coupled to nitrate reduction in the absence of iron was observed to be slow.[31] In the presence of nitrate-reducing and denitrifying microorganisms, enzymatic reduction of nitrate may produce nitrite (NO_2^-), nitrous oxide (N_2O), or nitric oxide (NO) species that may serve as abiotic oxidants for UO_2(s) and co-occur with direct enzymatic oxidation of U(IV) by anaerobic, nitrate-reducing bacteria.

Thiobacillus denitrificans is a widely distributed and well-characterized obligate chemolithoautotroph with a diverse metabolism[32] that is capable of anaerobic, nitrate-dependent U(IV) oxidation at circumneutral pH, as well as nitrate-dependent Fe(II) oxidation and coupled oxidation of inorganic sulfur compounds, under either aerobic or denitrifying conditions.[18,32−37] Beller[18] found that *T. denitrificans* was capable of anaerobic, nitrate-dependent oxidative dissolution of synthetic and biogenic U(IV) oxides in batch laboratory experiments; comparable U(IV) oxidation was not observed in killed controls or in no-nitrate controls with live cells. The role of denitrification intermediates (NO_2^-, NO, and N_2O) was not explicitly investigated in that study, although nitrite was not detected (detection limit, 10 μM) throughout the U(IV) oxidation experiment or in no-U(IV) controls that consumed 13 mM nitrate in 2 h. Biochemical studies of *T. denitrificans* insertion mutants[38] strongly suggest that, at least for this bacterium, direct enzymatic U(IV) oxidation under denitrifying conditions may have primacy over secondary abiotic U(IV) oxidation by denitrification intermediates such as nitrite. A mutant strain with a defective *Tbd_0187* gene (*Tbd_0187*::*kan*, also used in the present study) had only 47% of wild-type U(IV) oxidation activity and 64% of wild-type denitrification activity. However, when this mutant was complemented with an intact copy of the mutated gene (in *trans*, on a plasmid), the U(IV) oxidation activity was restored to 130% of wild-type levels but denitrification activity was not improved (55% of wild-type).[38] These results suggest that the presence of the intact *c*-type cytochrome encoded by the *Tbd_0187* gene was more important for U(IV) oxidation than the level of denitrification activity.

Although previous studies examined the dissolution of synthetic and biogenic U(IV) oxide phases under a variety of conditions, quantification of reaction rates and comparisons between different studies are challenging due to differences in the experimental approach and in the reactant material.[39−42] Comparisons between abiotic rates measured under sterile conditions and those measured in the presence of U(IV)-oxidizing microorganisms are often complicated by different experimental conditions needed to stimulate or maintain microbial activity. This study differs from prior investigations in its direct comparison of U dissolution in the absence and presence of a U(IV)-oxidizing model bacterium, *T. denitrificans*, and the addition of dissolved nitrate, nitrite, or both using relatively simple reactant solutions (i.e., buffered pH and carbonate-free solutions). Furthermore, our experiments employed flow through a porous medium (ground quartz) with a low solution volume in a strictly anaerobic environment rather than a batch or tank system in which the solution:solid ratio is high. This flow-through system provided a more realistic water:solid ratio with the advantage of removing dissolved species that may influence the reaction rate or solubility of mineral phases[43] and thus better simulated the dynamic porewater flow regime of saturated subsurface environments.

MATERIALS AND METHODS

Biogenic UO_2(s) Synthesis. Multiple batches of U(IV)-oxide (hereafter referred to as UO_2(s)) were produced by reduction of dissolved U(VI) by *Shewanella oneidensis* strain MR-1 following published methods.[6,44] *S. oneidensis* was grown in lysogeny broth (LB) under aerobic conditions. Cells were separated by centrifugation and washed with a buffer containing 30 mM $NaHCO_3$, 20 mM PIPES, and 20 mM lactate (pH 6.3) under anaerobic conditions (10% H_2, 90% Ar headspace). Solids were resuspended in the same solution amended with 1500 μM of uranyl acetate. After U(VI) reduction and precipitation of UO_2(s), solid particles were cleaned by resuspending the solids in 1 M NaOH for 12 h. Solids were then centrifuged and resuspended in anaerobic hexane for 12 h to separate UO_2(s) from biomass. Finally, the solids were centrifuged and stored under anaerobic conditions in a 1 M $NaHCO_3$ solution. All cultures and subsequent experiments were maintained under strict anaerobic and sterile conditions.

Dissolution Experiments. Dissolution of UO_2(s) in column flow-through experiments in the absence or presence of *T. denitrificans* was performed under anaerobic conditions at room temperature (25 ± 1 °C) in an anaerobic glovebox (Type A, Coy Laboratory Products, Inc., Grass Lake, MI). The entire experimental setup (input and output solutions, peristaltic pump, flow-through reactors, and tubing) was enclosed in the glovebox and purged with a gas composition of 90% N_2 and 10% H_2. Ultrapure water (18.2 MΩ·cm, Milli-Q Plus, Millipore) used to prepare the input solutions was boiled before use to remove dissolved oxygen, cooled in the anaerobic glovebox, and left for at least 24 h before performing experiments. Oxygen partial pressure in the glovebox was continuously monitored with a gas analyzer (Model 10, Coy Laboratory Products) and read 0 ppm during the experiments. All materials (tubes, quartz, solutions, columns, etc.) were sterilized before each experiment and equilibrated in the anaerobic glovebox before use.

Flow-through column experiments were carried out by packing a mixture of UO_2(s) with ground natural quartz (~200−500 μm from Unimin, Inc. and treated to clean surface impurities) into either 1 mL (0.8-cm ID × 2-cm length) or 5 mL (1.3-cm ID × 4.5-cm length) polypropylene chromatography columns (SUPELCO) and protected from light exposure. The final mixtures contained average concentrations of 570 mg U kg^{-1} of quartz to 170 mg U kg^{-1} of quartz for the 1 and 5 mL columns, respectively. Influent solutions were filtered with a 0.2 μm polycarbonate filter (Millipore) at both the inlet and outlet ends of the column. Flow was directed upward in the experiments to minimize bubbles (e.g., N_2 from denitrification) and was controlled with an HPLC pump (Ismatec C.P. 78001-02), which had a variation of less than 3%. Influent flow rates were gravimetrically determined. Influent dissolved oxygen and pH were measured periodically with an electrode (Orion 081010MD for dissolved oxygen and Thermo Scientific Orion 9102DJWP for pH). In selected experiments, effluent pH was monitored in line with a Thermo Scientific Orion 9102DJWP pH electrode.

https://dx.doi.org/10.1021/acs.est.0c01019
Environ. Sci. Technol. 2020, 54, 8010−8021

For abiotic dissolution experiments, quartz and $UO_2(s)$ were mixed under anaerobic conditions, then 1 mL of 10 mM NaCl (pH 7) was added to the mixture and packed into columns. For biotic experiments, *T. denitrificans* cells were harvested anaerobically by centrifugation in sealed polycarbonate bottles, washed once under anaerobic conditions, and resuspended in anaerobic 10 mM NaCl (pH 7). The optical density at 600 nm (OD_{600}) of this solution was adjusted to 2 (ca. 1.8×10^9 cells mL^{-1}) by diluting with the same NaCl solution, 1 mL was added to the mixture of quartz and $UO_2(s)$, and the slurry was immediately loaded into the columns (details of the cultivation and incubation of *T. denitrificans* can be found in the Supporting Information). In order to confirm that the process was enzymatically mediated, in addition to wild-type *T. denitrificans*, a mutant *T. denitrificans* strain that was ∼50% defective in U(IV) oxidation activity (relative to wild-type) was used that had an insertion mutation in the *Tbd_0187* gene, which encodes a *c*-type cytochrome shown to be involved in anaerobic U(IV) oxidation.[38]

Influent solutions for dissolution experiments were prepared by mixing reagents (ACS-grade or better $NaNO_3$, $NaNO_2$, NaCl, and MOPS as a pH buffer) with the deoxygenated ultrapure water. Solutions were made with variable nitrate, nitrite, and chloride concentrations to maintain an approximately constant ionic strength (Table S1). The pH was adjusted to ∼7 by adding NaOH (2 M) (Table S1). Solids were reacted with influent solutions (Table S1) for ∼2−5 days and column effluent was collected using a multichannel fraction collector (Spectra/Chrom® CF-1).

Uranium Dissolution Rates. The $UO_2(s)$ dissolution rate, R (mol m^{-2} s^{-1}), was calculated according to the following expression (eq 1):[41,45]

$$R = \frac{[U]_{ss} \times Q}{V \times A \times [UO_{2(s)}]} \quad (1)$$

where, assuming that the U concentration in the input solution is zero and the U released is due to $UO_2(s)$ dissolution, $[U]_{ss}$ is the concentration (mol U L^{-1}) in the effluent solution at a steady state, A is the specific surface area (m^2 g^{-1}), V is the estimated pore volume (L), $[UO_2(s)]$ is the $UO_2(s)$ solid concentration in the reactor (g L^{-1}), and Q is the volumetric flow rate through the system (L s^{-1}) (Table S2). $[U]_{ss}$ is the average concentration of 20 or 100 or more pore volumes eluted for the 5 or 1 mL columns, respectively, over which the effluent U concentration varied ≤15%. The error associated with the dissolution rate was estimated by propagation of the uncertainty in each of the terms in eq 1 (Table S2) and ranged from 6−27%. The estimated error was dominated by the uncertainty of the mass concentration of U in the steady state ($[U]_{ss} \leq 15\%$) and the uncertainty of the mass measurements (2−24%).

Analytical Methods. Detailed information about aqueous and solid analytical methods is presented in the Supporting Information. Briefly, column effluent solutions were analyzed for total U by ICP-MS (Agilent 7500cs); the detection limit was 4.2×10^{-5} μM (10 ppt) and analytical precision was < ±5%. We attempted to measure U(VI) speciation by kinetic phosphorescence analysis (KPA), but concentrations were below detection after dilution to reduce quenching from dissolved ions. Nitrate and nitrite were determined spectrophotometrically with a Cary-300-Bio spectrophotometer. $UO_2(s)$ was characterized by X-ray diffraction (XRD) on a PANalytical X'pert Pro diffractometer. Scanning electron microscopy (SEM) and transmission electron microscopy (TEM) images were obtained using a FEI Quanta 200 ESEM and a JEOL-JEM-2010 HRTEM, respectively. The surface area was measured using 7-point N_2 adsorption isotherms with a Micromeritics Tri-Star 3000 surface area analyzer. Uranium L_{III}-edge X-ray absorption spectroscopy (XAS) data, including X-ray absorption near edge structure (XANES) and extended X-ray absorption fine structure (EXAFS) spectra, were collected at the Stanford Synchrotron Radiation Lightsource (SSRL, California, USA) on beamlines 11−2 and 4−1.

RESULTS

Characterization of Unreacted Biogenic $UO_2(s)$. Powder XRD patterns of biogenic $UO_2(s)$ showed weak reflections that matched the major reflections of crystalline $UO_2(s)$ but with significant broadening, lower amplitude, and lower signal-to-noise ratio (Figure S1). These features are similar to those of biogenic $UO_2(s)$ produced in other studies and are attributed to small particle size, low crystallinity, and/or structural disorder.[6,46] The surface area of freeze-dried $UO_2(s)$ was measured by the N_2-BET method on two batches of $UO_2(s)$ (Table S1), with a mean surface area of 72.81 ± 0.69 m^2g^{-1}. Examination of unreacted $UO_2(s)$ particles by SEM showed particle aggregates of up to several micrometers in diameter (Figures S2a,b). Lattice fringes of particles observed by TEM images indicated individual particles of 2−4 nm in diameter (Figure S2c), consistent with other studies of biogenic $UO_2(s)$ produced by the method described above.[41] Results from XRD and TEM, and from XAS analysis (discussed below), support the interpretation that the majority of the biogenic starting material was mostly nanoparticulate $UO_2(s)$.

Flow-Through Column Abiotic Experiments. The abiotic dissolution of $UO_2(s)$ was examined in the presence of nitrate and/or nitrite (0−20 mM) in buffered solutions at circumneutral pH (7.0−7.3). Total U concentrations in the column effluent normalized to the total molar mass of $UO_2(s)$ added to the column in the abiotic experiments are shown in Figure 1. At the beginning of all the experiments, an initial peak of effluent U was observed, which is a common phenomenon in flow-through experiments that has been attributed to labile U(VI) on the UO_2 surface[47] or to the passage of colloidal U through the filter membrane during the first flush.[41] Therefore, the dissolution rate was calculated once a steady state in effluent U concentration was attained. The results display differences in the total amount of U released, and therefore in the amount of U dissolved, depending on the influent composition (Figure 1, Table S2). In the absence of an oxidant, the effluent U in replicate columns with anaerobic NaCl solutions buffered at pH ∼ 7 remained low and relatively constant (Figure 1a). The calculated average U dissolution rate (1.05×10^{-14} mol m^{-2} s^{-1}) is similar to the lowest rate reported by Ulrich et al.[41] for biogenically precipitated $UO_2(s)$ (Table 1). The addition of 20 mM nitrate to the influent solution resulted in an increase in the average dissolution rate (3.02×10^{-14} mol m^{-2} s^{-1}) compared to that of the experiments in the absence of an oxidant (Figure 1b). In contrast, when the columns were supplied with nitrite, the mass-normalized U effluent concentrations and calculated steady-state dissolution rates were higher than those in the presence of nitrate alone (Figure 1, Table S2). The dissolution rates with mixtures of nitrate and nitrite were similar to those

https://dx.doi.org/10.1021/acs.est.0c01019
Environ. Sci. Technol. 2020, 54, 8010−8021

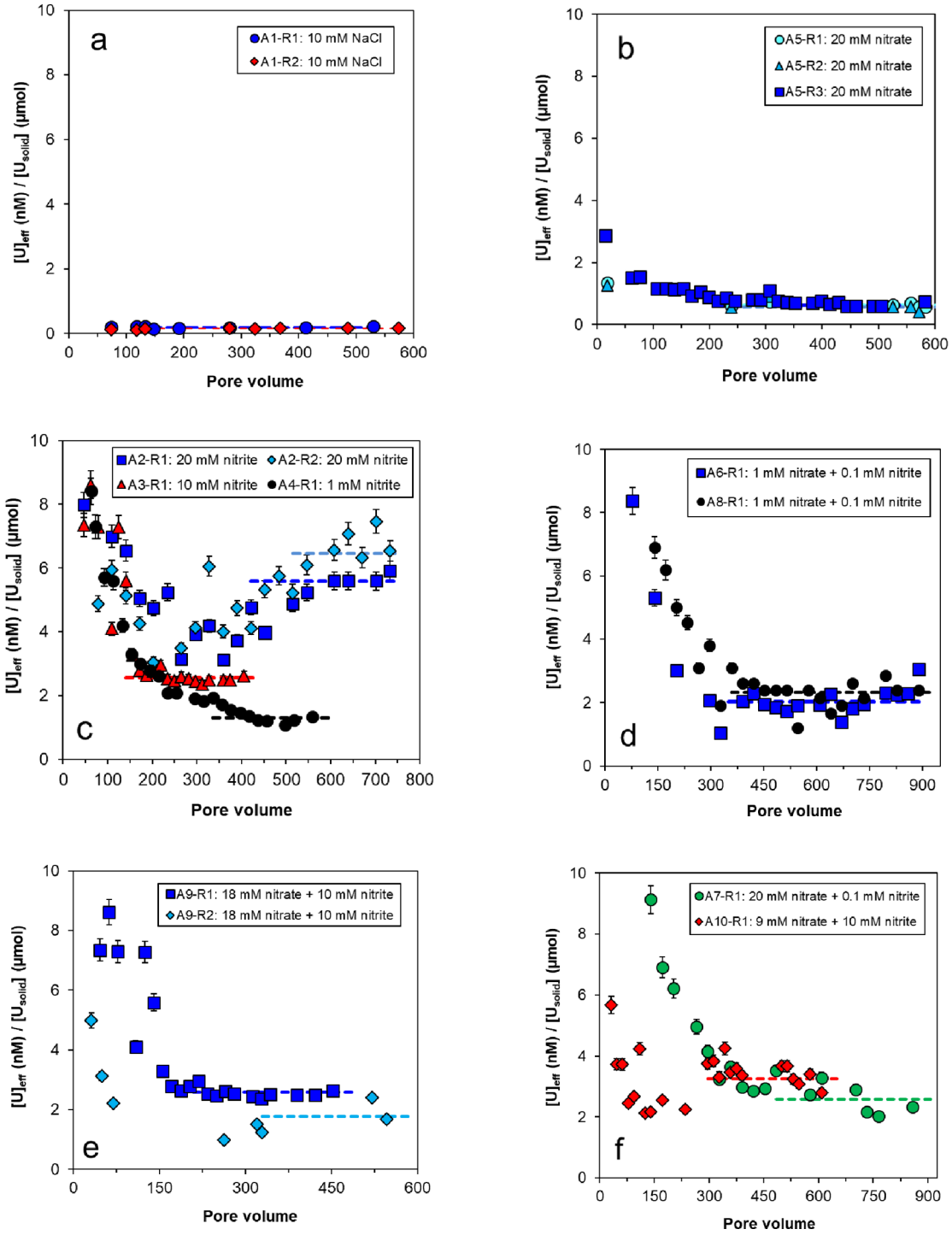

Figure 1. Uranium released in column experiments normalized by the initial U mass as a function of pore volume (a) without oxidant; (b) with NO_3^-; (c) with NO_2^-; and (d–f) with a mixture of NO_3^- and NO_2^-. Error bars correspond to the analytical uncertainty in measured U concentration. Dashed lines represent the steady-state values for each experiment used to calculate the U dissolution rate. Initial flush-out of high U is not shown.

obtained with nitrite only, which is consistent with the expected stronger effect of nitrite as an oxidant in abiotic $UO_2(s)$ dissolution compared to nitrate (Figure 1d–f, Figure S3, Table S2).

Flow-Through Column Experiments in the Presence of *T. denitrificans*. Dissolution of $UO_2(s)$ in the presence of *T. denitrificans* and dissolved nitrate (± nitrite) was compared to abiotic rate experiments. Replicate experiments always included an abiotic control column run simultaneously with the same influent solution as the biotic columns (Table S2). In most experiments, columns with *T. denitrificans* showed rates of $UO_2(s)$ dissolution of about one order-of-magnitude faster than those of the simultaneous abiotic control experiments (Figure 2, Table S2). However, in a few simultaneous replicate columns, $UO_2(s)$ dissolution rates were lower and closer to those of abiotic controls (e.g., B1-R2, B2-R3, and B4-R1, Table

https://dx.doi.org/10.1021/acs.est.0c01019
Environ. Sci. Technol. 2020, 54, 8010–8021

Table 1. Experiment Type, Influent Solutions, and UO_2(s) Dissolution Rates Obtained in this Work and Previous Studies under Anaerobic Conditions

UO_2(s)	type of experiment	pH	influent electrolyte	rate (mol m^{-2} s^{-1})	log rate (mol m^{-2} s^{-1})	experiment	replicates	reference
bio-UO_2	flow-through column	7.0–7.3	10 mM NaCl	$1.05 \times 10^{-14} \pm 2.67 \times 10^{-15}$	−13.98 ± 0.11	A1	R1, R2	this work
			abiotic, 1 mM NO_2^-	$1.66 \times 10^{-13} \pm 3.81 \times 10^{-14}$	−12.78 ± 0.10	A4	R1	
			abiotic, 10 mM NO_2^-	$1.64 \times 10^{-13} \pm 2.98 \times 10^{-14}$	−12.78 ± 0.08	A3	R1	
			abiotic, 20 mM NO_2^-	$4.11 \times 10^{-13} \pm 1.11 \times 10^{-13}$	−12.39 ± 0.12	A2	R1, R2	
			abiotic, 1 mM NO_3^- + 0.1 mM NO_2^-	$1.30 \times 10^{-13} \pm 2.61 \times 10^{-14}$	−12.89 ± 0.09	A6	R1	
			abiotic, 1 mM NO_3^- + 1 mM NO_2^-	$1.49 \times 10^{-13} \pm 3.33\times 10^{-14}$	−12.83 ± 0.10	A8	R1	
			abiotic, 20 mM NO_3^- + 0.1 mM NO_2^-	$1.65 \times 10^{-13} \pm 2.62 \times 10^{-14}$	−12.78 ± 0.09	A7	R1	
			abiotic, 9 mM NO_3^- + 10 mM NO_2^-	$2.09 \times 10^{-13} \pm 4.09 \times 10^{-14}$	−12.67 ± 0.08	A10	R1	
			abiotic, 18 mM NO_3^- + 10 mM NO_2^-	$1.55 \times 10^{-13} \pm 4.71 \times 10^{-14}$	−12.81 ± 0.14	A9	R1, R2	
			abiotic, 1 mM NO_3^- + 0.08 mM NO_2^-	$1.15 \times 10^{-14} \pm 1.60 \times 10^{-15}$	−13.94 ± 0.06	B4	CT7	
			abiotic, 4 mM NO_3^-	$2.93 \times 10^{-14} \pm 6.70 \times 10^{-15}$	−13.53 ± 0.10	B1	CT3	
			abiotic, 5 mM NO_3^-	$2.51 \times 10^{-14} \pm 6.68 \times 10^{-15}$	−13.60 ± 0.12	B2	CT4	
			abiotic, 10 mM NO_3^-	$4.61 \times 10^{-14} \pm 1.40 \times 10^{-14}$	−13.34 ± 0.13	B3a, B3b, B5	CT5, CT6, CT8	
			abiotic, 20 mM NO_3^-	$3.02 \times 10^{-14} \pm 1.03 \times 10^{-14}$	−13.52 ± 0.15	A5	R1, R2, R3	
			Td +1 mM NO_3^- + 0.08 NO_2^-	$1.12 \times 10^{-13} \pm 5.63 \times 10^{-14}$	−12.95 ± 0.18	B4	R1, R2, R3	
			Td + 4 mM NO_3^-	$2.35 \times 10^{-13} \pm 8.06 \times 10^{-14}$	−12.63 ± 0.12	B1	R1, R2, R3	
			Td + 5 mM NO_3^-	$2.44 \times 10^{-13} \pm 7.10 \times 10^{-14}$	−12.61 ± 0.10	B2	R1, R2, R3	
			Td + 10 mM NO_3^-	$3.41 \times 10^{-13} \pm 8.05 \times 10^{-14}$	−12.47 ± 0.10	B3b	R1, R2, R3	
			Td mutant + 10 mM NO_3^-	$1.91 \times 10^{-13} \pm 5.50 \times 10^{-14}$	−12.72 ± 0.13	B5	R1, R2, R3	
synthetic UO_2[c]	flow-through	7–11	8 mM $NaClO_4$	1.90×10^{-12}	−11.72 ± 0.02			Bruno et al.[39]
synthetic UO_2	flow stirred tank reactor	7.50	10 mM $NaClO_4$	7.50×10^{-13}	−12.12 ± 0.02			Frazier et al.[42]
bio-UO_2	flow-through	7.60	1 mM HEPES	9.85×10^{-14}	−13.01			Ulrich et al.[41]
		7.25	1 mM HEPES	3.42×10^{-13}	−12.47			
		7.67	1 mM HEPES	1.07×10^{-14}	−13.97			
synthetic UO_2[c]		8.00	1 mM NaNO3, TAPS	4.03×10^{-12}	−11.39			
		7.70	1 mM HEPES	5.51×10^{-13}	−12.26			
		7.25	1 mM HEPES	2.80×10^{-13}	−12.55			
		7.00		2.15×10^{-12}	−11.72 ± 0.24[d]			

[a] *Td: Thiobacillus denitrificans* wild type. [b] *Td mutant: Thiobacillus denitrificans* mutant. [c] A thin film was used. [d] Calculated at pH 7 from the kinetic rate law obtained by Ulrich et al.[41] under reducing conditions for pH range 3–8.

S2). In addition, nitrite concentrations (Figure S4) were below the detection limit (B1-R2), slightly lower (B2-R3) than the biotic replicates, or followed the same trend as the control experiment (B4-R1), which could indicate low or no enzymatic oxidation. Overall, UO_2(s) dissolution rates were more variable in experiments with *T. denitrificans* than in abiotic experiments, and a relatively constant effluent U concentration was sometimes not observed until near the end of the experiment. Nitrite concentrations measured in the effluent solutions of experiments involving *T. denitrificans* with nitrate (but no added nitrite) were higher (~20–160 μM) than those in abiotic nitrate control experiments (~5–10 μM), demonstrating microbially accelerated conversion of nitrate to nitrite (Figure S4). Furthermore, in two control column experiments with *T. denitrificans* and quartz but no UO_2(s), solutions with influent nitrate concentrations of 1 or 10 mM produced effluent nitrite concentrations near the limit of detection (0.42 μM) (data not shown). Overall, abiotic dissolution rates measured in experiments with added nitrite were similar to rates observed in experiments with *T. denitrificans* and added nitrate (Table 1).

Column experiments were performed with a mutant strain of *T. denitrificans* that was previously shown to be ~50% defective in U(IV) oxidation.[38] Results showed a decrease of 44% in the average UO_2(s) dissolution rate compared to that of experiments with the wild-type strain. The decrease in the dissolution rate was smaller (34% rather than 44%) if effluent U concentrations were compared with those of simultaneous abiotic control columns with the same influent nitrate concentration (10 mM) (e.g., controls B3b-CT6 and B5-

https://dx.doi.org/10.1021/acs.est.0c01019
Environ. Sci. Technol. 2020, 54, 8010–8021

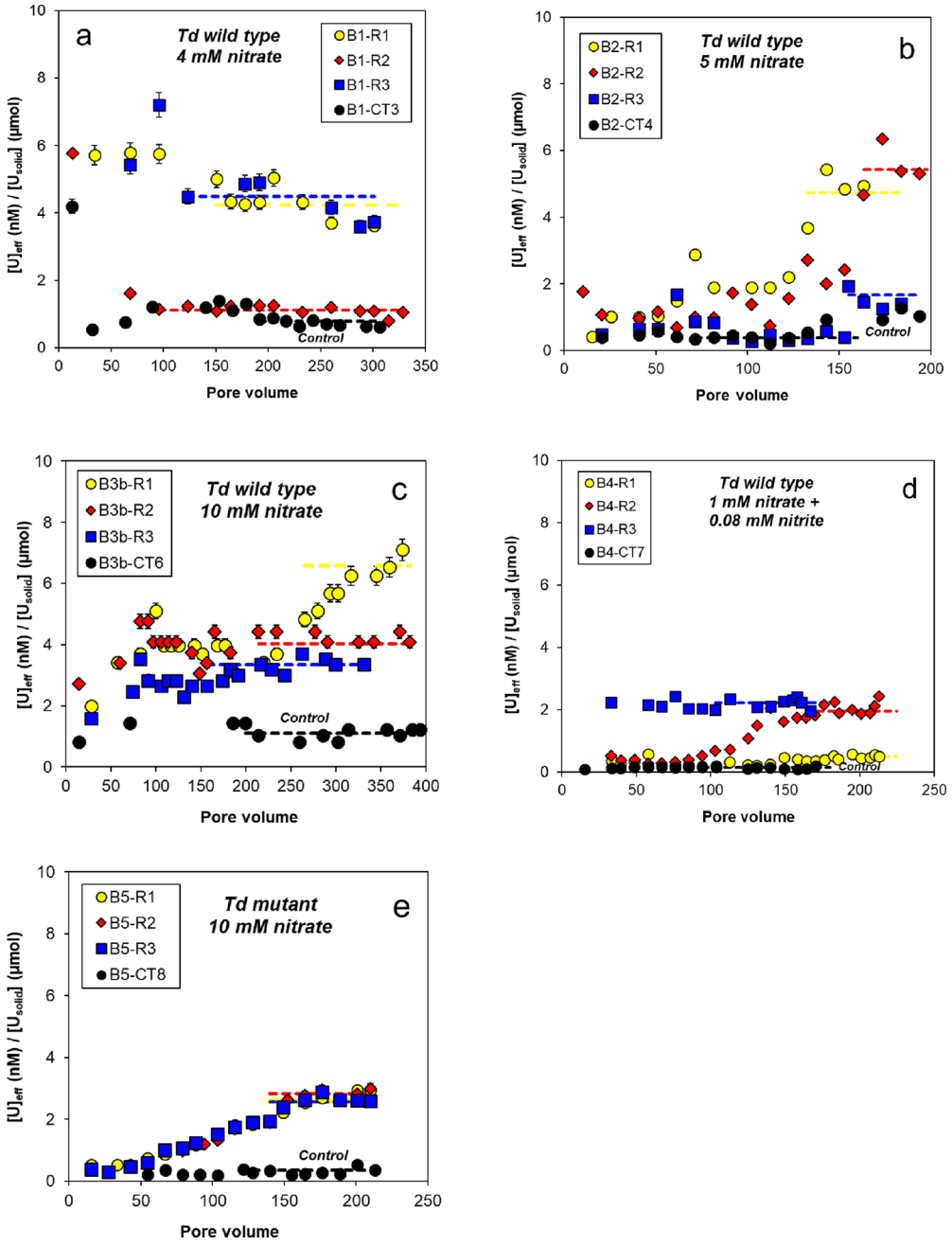

Figure 2. Uranium released in column experiments normalized by the initial U mass as a function of pore volume in the presence of wild-type *T. denitrificans* and (a) 4 mM NO_3^-; (b) 5 mM NO_3^- (c) 10 mM NO_3^-; (d) 1 mM NO_3^- and 0.08 mM NO_2^-; and (e) 10 mM NO_3^- and a *T. denitrificans* mutant strain (*Tbd_0187*::*kan*) ~50% defective in U(IV) oxidation, compared to simultaneous abiotic control experiments without *T. denitrificans* (black circles). Error bars correspond to the analytical uncertainty in measured U concentration. Dashed lines represent the steady-state values for each experiment used to calculate the U dissolution rate. Initial flush-out of high U is not shown.

CT8 in Figure 2c,e, respectively) (Table 1, Figure 2). The differences in rate exceeded the estimated propagated error for these experiments (Table 1). This result supports the role of enzymatic mediation by *T. denitrificans* in the U(IV) oxidation process (Figure 2).

X-Ray Absorption Spectroscopy of Unreacted and Reacted UO_2(s). Because of the low concentrations of U and the presence of quartz in the reacted columns (which added background noise), XAS data were limited to mostly XANES spectra, with usable EXAFS spectra obtained for only three reacted samples. XANES spectra of UO_2(s) samples and reference compounds at the U L_{III}-edge are shown in Figure S5. The absorption maximum for U(IV) is found at 17,176 eV, which is ~2.7 eV lower in energy than the maximum for U(VI). U(VI)-oxide compounds show a shoulder at approximately 17,191 eV, which has previously been shown to result from multiple scattering resonances of the linear uranyl ion structure, specifically due to the short U-O_{ax} bonds.[48,49] Best fits of linear combinations of unreacted UO_2(s) and schoepite $[(UO_2)_8O_2(OH)_{12}\cdot 12(H_2O)]$ as a U(VI) reference compound showed that spectra were dominated by the unreacted material (72−100% ±10% in normalized spectra) with a small fraction of U(VI) present in the solids (Figure S5, Table 2). Experiments performed with

https://dx.doi.org/10.1021/acs.est.0c01019
Environ. Sci. Technol. 2020, 54, 8010−8021

Table 2. Linear Combination Fit (LCF) Results for U L_{III} XANES for a Control Experiment without Oxidant (CT0), and for Biogenic UO_2(s) Samples after Dissolution Experiments under Abiotic (*A* Samples) Conditions and in the Presence of *T. denitrificans* (*B* Samples)

		model fit (%)[a]			goodness-of-fit[b]	normalized fit (%)[c]	
sample	oxidant	U(IV)	U(VI)	Total		U(IV)	U(VI)
CT0[d]	no oxidant	100	0	100	0.002	100	0
A2	20 mM NO_2^-	77	26	103	0.004	75	25
A5	20 mM NO_3^-	98	0	98	0.004	100	0
A6	1 mM NO_3^- + 0.1 mM NO_2^-	88	9	98	0.002	90	10
A8	1 mM NO_3^- + 1 mM NO_2^-	89	13	102	0.002	88	12
A9(R2)	18 mM NO_3^- + 10 mM NO_2^-	85	15	100	0.001	85	15
B1(R1)	4 mM NO_3^-	76	13	89	0.007	85	15
B1(R2)	4 mM NO_3^-	75	29	103	0.018	72	28
B2(R1)	5 mM NO_3^-	77	17	94	0.003	82	18
B2(R2)	5 mM NO_3^-	78	15	93	0.006	83	17
B3b(R1)	10 mM NO_3^-	88	9	97	0.004	91	9
B3b(R2)	10 mM NO_3^-	73	26	98	0.009	74	26

[a]End members used for LCF were biogenic UO_2(s) (unreacted sample Unr-1) for U(IV) and schoepite ($(UO_2)_8O_2(OH)_{12}\cdot 12(H_2O)$) for U(VI). [b]*R* factor = Σ(data-fit)$^2/\Sigma$(data)^2. [c]The percentage of U components is normalized to a sum of 100%. [d]Batch control experiment with biogenic UO_2(s) and 10 mM sodium acetate (no oxidant). Data and fits shown in Supporting Information Figure S5.

nitrite had the highest uranyl fraction among the abiotic samples analyzed by XAS, although results were variable among all columns. For columns reacted in the presence of *T. denitrificans*, the highest U(VI) fractions (28% U(VI) in B1(R2) and 26% U(VI) in B3b(R2)) were found in experiments with nitrate (4 or 10 mM, respectively) that were run for longer duration (cumulative fluid volumes of 647 and 776 mL, respectively; Table S2), although fit results were again variable.

Quantitative fits of EXAFS spectra of two unreacted UO_2(s) samples (Unr-1 and Unr-3) indicated a local atomic environment around U consistent with the UO_2(s) structure[6] (Figure 3, Table S3). As noted in prior studies, atomic backscattering amplitudes in EXAFS of biogenic nanoparticulate UO_2(s) tend to be lower than those in crystalline U compounds, particularly for atoms beyond the first bonded shell of O atoms due to small particle size, local disorder, and in some cases a component of monomeric U(IV) species.[50,6,8,51,9,23] Backscattering from U−U shells at interatomic distances of ∼5.46 and 6.73 Å were not significant in the EXAFS spectrum of Unr-1 but were fit in Unr-3 (Figure 3), which may indicate small differences in particle size or crystallinity and/or a variable fraction of monomeric U(IV), a common product of enzymatic U(VI) reduction in the natural environment[52−54] and laboratory studies,[55] in addition to nanoparticulate UO_2(s).[50,8,51,23] In reacted column samples, XANES analysis indicated a low fraction of U(VI) (<30%), so the three EXAFS spectra were examined for evidence of backscattering from near-neighbor axial oxygen atoms (O_{ax}) in the uranyl group (UO_2^{2+}) at interatomic distances from ∼1.74 to 1.83 Å (Table S4), in addition to O atoms at distances indicative of unreacted UO_2(s) (2.30−2.35 Å). Quantitative EXAFS fits of reacted samples A2 (abiotic with 20 mM nitrite) and B2 (with *T. denitrificans* and 5 mM nitrate) showed no evidence of O_{ax} backscattering or U−O backscattering at distances other than expected for U−O in UO_2(s). Fit results were similar to those found for the U−O and U−U shells for Unr-1 and Unr-3 (Table S3). In the EXAFS fit of reacted sample A9(R2) (abiotic with 18 mM nitrate +10 mM nitrite), weak backscattering from O_{ax} (at 1.77 Å) was permissible although backscattering at distances characteristic of U(VI) and equatorial O atoms ($U-O_{eq}$), which span a range of distances, could not be distinguished in the fit from O atoms in UO_2(s) (Figure 3, Table S3). This column was reacted at a high nitrate

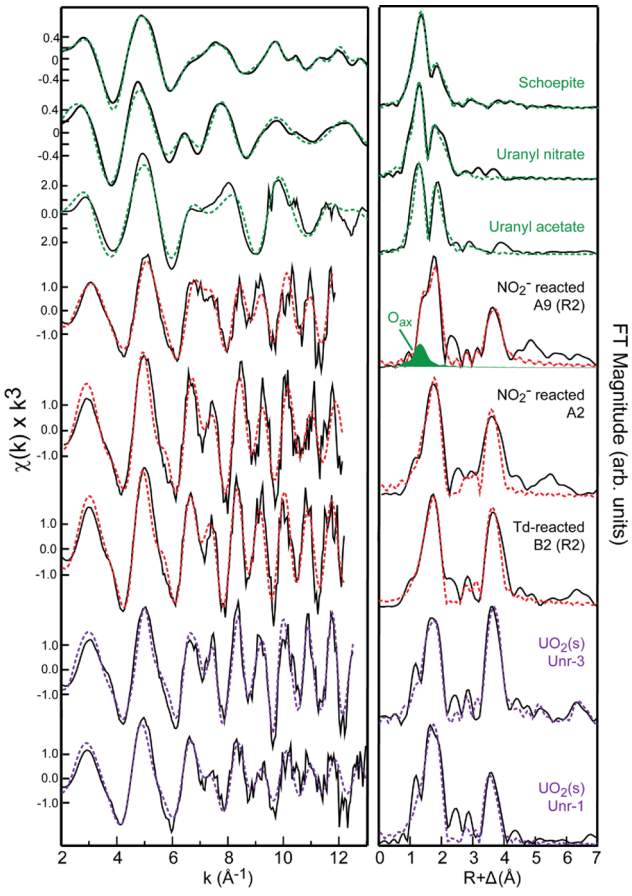

Figure 3. Uranium L_{III} EXAFS spectra and Fourier transforms (FTs) of unreacted UO_2(s) samples (Unr-1 and Unr-3), reacted samples (B2(R2), A2, and A9(R2)), and U(VI) reference compounds (uranyl acetate, uranyl nitrate, and schoepite). Overlapping dashed lines represent the nonlinear least-squares shell-by-shell fits (numerical fit results shown in Tables S4 and S5).

https://dx.doi.org/10.1021/acs.est.0c01019
Environ. Sci. Technol. 2020, 54, 8010−8021

+ nitrite concentration (28 mM) and with a higher cumulative pore volume than abiotic column A2 (285 vs 220 mL). Overall, the XAS results showed that U in reacted columns mostly resembled unreacted UO_2(s) but suggested evidence for a minor fraction of U(VI), with slightly more U(VI) at high oxidant concentrations and longer reaction times. The lack of molecular-scale evidence for interatomic scattering indicative of uranyl oxyhydroxide minerals suggests the formation mostly of U(VI) surface complexes. If U(VI)-oxide solid phases were present, their fraction was below detection by XAS.

DISCUSSION

Abiotic and Biotic Rates of Anaerobic UO_2(s) Dissolution. Dissolution rates of UO_2(s) at steady-state U release as a function of nitrate and nitrite concentration and in the absence and presence of *T. denitrificans* are compiled in Figure 4. In the absence of an oxidant, the average UO_2(s) dissolution rate (1.05×10^{-14} mol m^{-2} s^{-1}) was similar to the slowest rates published previously for bio-UO_2(s) at neutral pH in carbonate-free solutions (1.07×10^{-14} to 3.42×10^{-13} mol m^{-2} s^{-1})[41] (Table 1). Abiotic dissolution of UO_2(s) by nitrate alone was relatively slow (2.51×10^{-14} to 4.61×10^{-14} mol m^{-2} s^{-1}), although slightly faster than without addition of an oxidant, and not dependent on nitrate concentration (4−20 mM NO_3^-) (Figure 4). These rates, measured at pH 7.0−7.3, are approximately two orders of magnitude slower than the rate reported by Ulrich et al.[41] for dissolution of synthetic UO_2(s) in the presence of 1 mM nitrate at pH 8 (4.03×10^{-12} mol m^{-2} s^{-1}; Table 1). Ulrich et al.[41] obtained slower dissolution rates for bio-UO_2 than for synthetic UO_2 solids (Table 1), although these differences were estimated to be within their experimental error. With the addition of nitrite as an oxidant (with or without nitrate), UO_2(s) dissolution rates were approximately 5 to 10 times higher than with nitrate alone, with the exception of one experiment at low nitrite and nitrate concentrations (Figure 4, Figure S3, Table 1). Prior studies have pointed out that nitrite, a product of nitrate reduction, is more reactive than nitrate and could abiotically oxidize U(IV).[16,17] To our knowledge, however, no anaerobic UO_2(s) dissolution rates in the presence of nitrite under flow conditions have been reported previously. In the absence of microbial activity, our experiments show the ability of nitrite to accelerate UO_2(s) dissolution compared with nitrate, although there was not a strong dependence on influent nitrite concentration over the range used in our experiments (0.08−20 mM, Figure S3).

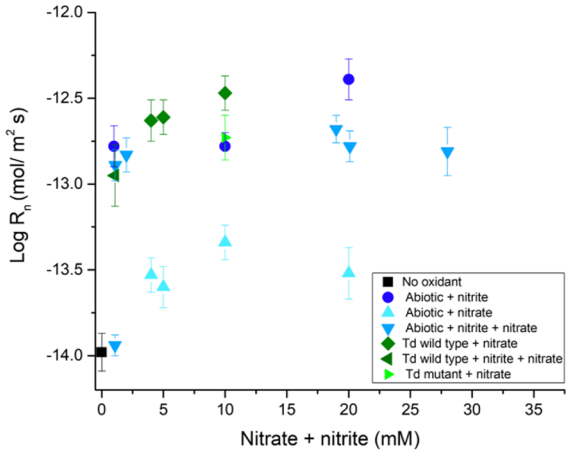

Figure 4. Log UO_2(s) dissolution rate vs oxidant concentration (no oxidant, black squares; NO_2^-, NO_3^-, or a mixture of NO_3^- and NO_2^-) in the absence (abiotic experiments, blue symbols) or presence of *T. denitrificans* (Td wild-type and Td mutant, green symbols). The error was estimated by propagation of experimental uncertainties and dominated by the variation in effluent U concentration at steady state ($[U]_{ss} \leq 15\%$) and the uncertainty of the U mass measurements (0.5−25%).

Rates of UO_2(s) dissolution in the presence of *T. denitrificans* with nitrate (and with 0.08 mM nitrite in one set of experiments) were generally higher than those for abiotic experiments with nitrate only but similar to the range observed for abiotic experiments with nitrite (Figure 4). Experiments with a mutant strain of *T. denitrificans* that is partially defective in U(IV) oxidation[38] showed a decrease in the average dissolution rate compared to rates from experiments with wild-type *T. denitrificans* and the same concentration of influent nitrate, providing evidence of enzymatically catalyzed U(IV) oxidation by *T. denitrificans*. Effluent U concentrations in biotic experiments ranged from ∼1−40 nanomolar, compared to effluent nitrite of ∼5−150 micromolar from the reduction of nitrate, with no apparent correlation between effluent U and nitrite concentration, which was variable among biotic experiments (Figure S4). Therefore, U(IV) alone could not have served as the dominant electron donor for nitrate reduction by *T. denitrificans*. These observations support previously reported batch studies of UO_2(s) oxidation by *T. denitrificans* indicating that nitrate reduction is coupled to a primary electron donor other than U(IV) (e.g., H_2 from the glovebox atmosphere).[18] In fact, nitrate-dependent U(IV) oxidation catalyzed by *T. denitrificans* has been reported to have a cometabolic dependence on H_2 oxidation.[18]

Mechanisms of Anaerobic UO_2(s) Dissolution. Under anaerobic conditions in the absence of oxidants, radiolysis products such as H_2O_2 and O_2 from alpha decay of U reacting with water molecules can oxidize U(IV) to produce surface species of U(V) or U(VI).[22,41,56−59] In early studies, Bruno et al.[39] assumed that detachment of a hydroxo-U(IV) species ($(U(OH)_X^{(4-x)+})$) was the rate-determining step in thin-film, flow-through dissolution experiments of synthetic UO_2(s) under reducing conditions. In our experiments, U(IV) oxidation attributed to radiolysis should be relatively small given the short time scale (minutes to hours) but is probably not negligible. Total U concentration, rather than U species, was measured in effluent solutions, and therefore we do not have direct knowledge of U aqueous speciation. In the absence of an oxidant (experiments with NaCl solution), it is possible that U release from UO_2(s) surfaces was a combination of dissolved U(IV) and U(VI) species from the reaction with oxidants such as H_2O_2 from the radiolysis of water.

In anaerobic systems, the abiotic oxidation of UO_2(s) coupled to nitrate reduction is slow.[16,18] Slightly faster UO_2(s) dissolution rates in the presence of dissolved nitrate compared to experiments with NaCl only may be explained by adsorption of nitrate and direct oxidation of UO_2(s), or to radiolysis of nitrate to produce nitrite or other reactive NO_x species[60] at the UO_2(s) surface and acceleration of U(IV) oxidation and U(V) or U(VI) release. Both nitrate and chloride form weak complexes in solution with U(IV) of similar thermodynamic affinity (Table S5) and thus their sorption behavior on UO_2(s) is probably similar. Dissolution experiments showed no dependence on nitrate concentration, and XANES analysis of

https://dx.doi.org/10.1021/acs.est.0c01019
Environ. Sci. Technol. 2020, 54, 8010−8021

one abiotic sample (A5) reacted with 20 mM nitrate (and no nitrite or NaCl) showed only U(IV) in the solids after reaction. These observations indicate that direct U oxidation by nitrate, or radiolysis to nitrite (or other reduced N species) followed by U oxidation, is a weak effect. Aqueous complexes of U(IV) with nitrate or chloride are orders of magnitude weaker than U(IV)-hydroxo complexes (Table S5), and the latter are expected to be the stable U(IV) species detaching from the UO_2(s) surface in the absence of U oxidation.[39] Slightly faster UO_2(s) dissolution rates with nitrate compared to chloride at similar concentrations are indirect evidence of surface oxidative dissolution because, if detachment of U from the surface through the formation of U(IV)-hydroxo complexes was rate-determining, then the observed rates in the presence of either chloride or nitrate at constant pH should overlap. If nitrate adsorption accelerates surface oxidation of U(IV) to U(VI) by either of the mechanisms described above, then detachment of uranyl-hydroxo complexes would be rate-determining, and rates would be higher with more surface oxidation. This mechanism relies on surface enhancement of UO_2(s) dissolution, since the concentration of nitrate (1−20 mM) would be too low for radiolysis reactions to be important in bulk solution.[60] The lack of dependence of the dissolution rate on nitrate concentration is consistent with a surface mechanism that involves nitrate adsorption and detachment of an oxidized U product, perhaps in addition to a U(IV) species, but it is a relatively small effect overall (Figure 4).

Nitrite is a more effective oxidant of U(IV) than nitrate, with dissolution rates in abiotic experiments about 5 to 10 times faster than with nitrate, and similar to average rates measured in biotic experiments (Figure 4). In abiotic experiments with nitrite (± nitrate) or biotic experiments with nitrate, bulk XANES analysis indicated that a low fraction of total U (3−19%) was retained in the column as oxidized U(VI), with higher fractions (up to 32%) observed for experiments of longer duration. These results are consistent with the presence of some adsorbed or surface U(VI) or perhaps some U(V) that is not detectable by XANES.[22] EXAFS analysis showed the lack of formation of an oxidized U(VI) phase (e.g., schoepite) as a surface coating, which was proposed in other studies of UO_2(s) dissolution,[22,61] probably due to the short time scale of our experiments (3−5 days) and relatively slow rates of oxidation, or due to the mobilization of desorbed U(VI) species in our flow-through columns. The presence of surface U(VI) in similar proportions in both biotic and abiotic experiments, and the observation that dissolution rates are independent of nitrite concentration, support the hypothesis that the rate-determining step at steady-state release is detachment of oxidized U(VI) from the UO_2(s) surface rather than electron transfer or ion diffusion.

In *T. denitrificans,* two membrane-associated, *c*-type cytochromes that are involved in anaerobic U(IV) oxidation were previously identified by Beller et al.[38] The similarity between abiotic experiments with nitrite and biotic experiments with nitrate suggests a close interplay of molecular and enzymatic electron transfer among N and U species. In experiments with *T. denitrificans*, it is likely that U(IV) oxidation takes place via both the membrane-associated *c*-type cytochrome (enzymatic) pathway previously described[38] and as a secondary abiotic reaction with denitrification intermediates (e.g., nitrite, nitric oxide, and/or nitrous oxide), with the relative proportions of each pathway varying during the experiments. Steady-state rates were estimated from U effluent concentrations toward the end of the experiments after formation of a fraction of U(VI) in the columns (detected by XAS), presumably as a surface species. The observed biotic and nitrite-catalyzed rates in this study are similar to the dissolution rates measured for the uranyl oxyhydroxide minerals Na-compreignacite ($R = 3.71 \times 10^{-13}$ mol m^{-2} s^{-1}; log $R = -12.43$) and K-compreignacite ($R = 1.28 \times 10^{-13}$ mol m^{-2} s^{-1}; log $R = -12.89$) at pH 6.6−6.8 and low dissolved carbonate concentrations using a similar experimental setup of flow-through, quartz-packed columns.[62] In that study, the authors noted that despite ion exchange during the experiments, mineral dissolution rates were relatively insensitive to the interlayer cation identity because the molecular-scale rate-determining step was the detachment of the uranyl group from the mineral surface.[63−65] The similarity in observed rates may indicate that uranyl detachment from the surface is a common controlling mechanism when a steady-state surface concentration of oxidized U is achieved.

Environmental Implications. Reduced U forms, including crystalline uraninite and amorphous U(IV)-oxides, are susceptible to reoxidation[5,20,66,14] and pose challenges to long-term stability of U(IV) in aquifer sites remediated by reductive immobilization. This is mainly due to groundwater influxes continuously introducing U(IV)-oxidizing species (e.g., O_2, NO_3^-, and NO_2^-). Of these species, one of the most relevant for contaminated subsurface environments at nuclear sites is nitrate, a common co-contaminant with U at U.S. Department of Energy (DOE) sites.[16,24,67] Nitrate inputs to aquifers have been observed to threaten U(IV) stability, not only at nuclear sites but also in areas unaffected by nuclear activities.[28−30] Although O_2 is a stronger oxidant,[22,68,69] this study showed that oxidative dissolution of reduced U under anaerobic conditions is accelerated substantially by the addition of dissolved nitrite or by a denitrifying chemolithoautotroph, *T. denitrificans,* that is pervasive in aquifers and soils, together with nitrate (log rates from −13.94 to −12.31 mol m^{-2} s^{-1}). *T. denitrificans* or closely related species are prominent members of microbial communities at some U-contaminated sites.[18,70,71,37] In the environment, nitrite is a reactive, transient species that is produced primarily by microbial reduction of nitrate. In anaerobic aquifers with relatively high nitrate concentrations, the production of nitrite by nitrate-reducing microorganisms, together with enzymatically catalyzed, nitrate-dependent U(IV) oxidation, are likely dual processes by which reduced U solids may be oxidized and mobilized in the aqueous phase. Steady-state dissolution rates appear to be controlled by U(VI) detachment and release to solution as the rate-determining step once surface-oxidized U(VI) species form on UO_2(s) particle surfaces. Initial dissolution rates, which were not considered in this study and may involve release of both U(IV) and U(VI) species, are more likely to be controlled by electron transfer processes involving microbial enzymatic oxidation of U(IV) and reduction of nitrate, and by surface adsorption, complexation, and U(IV) oxidation.[22,41] If a steady-state concentration of surface-oxidized U species develops, the overall rate of U release to solution may be similar to that of uranyl oxyhydroxide minerals and thus would be strongly controlled by pH and dissolved carbonate concentration.[62] In natural groundwater, the presence of dissolved inorganic carbon, an ubiquitous component of groundwater, would promote the removal of surface U(VI) by formation of uranyl-carbonate complexes,[22,62] increasing U mobility. Our findings improve our understanding of U(IV)

https://dx.doi.org/10.1021/acs.est.0c01019
Environ. Sci. Technol. 2020, 54, 8010−8021

oxidation and remobilization processes in nitrate-contaminated aquifers and will contribute to predictive modeling and strategies for mitigating U mobilization.

■ ASSOCIATED CONTENT

Supporting Information

The Supporting Information is available free of charge at https://pubs.acs.org/doi/10.1021/acs.est.0c01019.

Methods; XRD biogenic $UO_2(s)$; SEM and TEM images of biogenic $UO_2(s)$; log $UO_2(s)$ dissolution rate vs influent nitrite concentration; nitrite effluent concentrations in the experiments performed in the presence of *T. denitrificans* and nitrate; uranium L_{III} XANES spectra and LCF of the first derivative of spectra; experimental conditions for dissolution experiments and solid analyses performed before and after the reaction; experimental conditions and $UO_2(s)$ dissolution rates based on steady-state values; uranium L_{III} EXAFS fit results of biogenic $UO_2(s)$ spectra; uranium L_{III} EXAFS fit results of reference compound spectra; and stability constants for selected U(IV) complexes (PDF)

■ AUTHOR INFORMATION

Corresponding Author

Maria P. Asta − *Sierra Nevada Research Institute, University of California Merced, Merced, California 95343, United States;* orcid.org/0000-0001-6502-6744; Email: Maria-Pilar.Asta-Andres@univ-grenoble-alpes.fr

Authors

Harry R. Beller − *Lawrence Berkeley National Laboratory, Berkeley, California 94720, United States; Department of Chemical Engineering and Applied Chemistry, University of Toronto, Toronto, Ontario M5S 3E5, Canada;* orcid.org/0000-0001-9637-3650

Peggy A. O'Day − *Sierra Nevada Research Institute and Department of Life and Environmental Sciences, University of California Merced, Merced, California 95343, United States;* orcid.org/0000-0002-8698-5159

Complete contact information is available at: https://pubs.acs.org/10.1021/acs.est.0c01019

Notes

The authors declare no competing financial interest.

■ ACKNOWLEDGMENTS

This study was supported by the Subsurface Biogeochemistry Research Program, U.S. Department of Energy, Office of Science, Office of Biological and Environmental Research [award no. DE-FG02- 08ER64614 (UC Merced) and DE-AC02-05CH11231 (LBNL)]. Portions of this research were carried out at the Stanford Synchrotron Radiation Lightsource at the SLAC National Accelerator Laboratory, an Office of Science User Facility operated for the U.S. Department of Energy Office of Science by Stanford University. Use of the Stanford Synchrotron Radiation Lightsource, SLAC National Accelerator Laboratory, is supported by the U.S. Department of Energy, Office of Science, Office of Basic Energy Sciences under Contract No. DE-AC02-76SF00515. We thank Peng Zhou, Nelson Rivera, Virginia Illera, Harshani Peiris, Jesus Luna, Jesus Ciriza, Chi-Shuo Chen, Kennedy Nguyen, Gayatri Premshekharan, Masakazu Kanematsu, and Estela Reinoso Maset for assistance. The authors thank M. Dunlap, Imaging and Microscopy Facility (UC Merced), for assistance with XRD and electron microscopy, and L. Zhao, Environmental Analytical Laboratory (UC Merced), for analytical support.

■ REFERENCES

(1) Lovley, D. R.; Phillips, E. J. P.; Gorby, Y. A.; Landa, E. R. Microbial reduction of uranium. *Nature* **1991**, *350*, 413−416.

(2) Lovley, D. R.; Phillips, E. J. Reduction of uranium by *Desulfovibrio desulfuricans*. *Appl. Environ. Microbiol.* **1992**, *58*, 850−856.

(3) Williams, K. H.; Bargar, J. R.; Lloyd, J. R.; Lovley, D. R. Bioremediation of uranium-contaminated groundwater: A systems approach to subsurface biogeochemistry. *Curr. Opin. Biotechnol.* **2013**, *24*, 489−497.

(4) Anderson, R. T.; Vrionis, H. A.; Ortiz-bernad, I.; Resch, C. T.; Long, P. E.; Dayvault, R.; Karp, K.; Marutzky, S.; Metzler, D. R.; Peacock, A.; White, D. C.; Lowe, M.; Lovley, D. R. Stimulating the in situ activity of *Geobacter* species to remove uranium from the groundwater of a uranium-contaminated aquifer. *Appl. Environ. Microbiol.* **2003**, *69*, 5884−5891.

(5) Alessi, D. S.; Lezama-Pacheco, J. S.; Janot, N.; Suvorova, E. I.; Cerrato, J. M.; Giammar, D. E.; Davis, J. A.; Fox, P. M.; Williams, K. H.; Long, P. E.; Handley, K. M.; Bernier-Latmani, R.; Bargar, J. R. Speciation and reactivity of uranium products formed during in situ bioremediation in a shallow alluvial aquifer. *Environ. Sci. Technol.* **2014**, *48*, 12842−12850.

(6) Schofield, E. J.; Veeramani, H.; Sharp, J. O.; Suvorova, E.; Bernier-Latmani, R.; Mehta, A.; Stahlman, J.; Webb, S. M.; Clark, D. L.; Conradson, S. D.; Ilton, E. S.; Bargar, J. R. Structure of biogenic uraninite produced by *Shewanella oneidensis* strain MR-1. *Environ. Sci. Technol.* **2008**, *42*, 7898−7904.

(7) Burgos, W. D.; McDonough, J. T.; Senko, J. M.; Zhang, G.; Dohnalkova, A. C.; Kelly, S. D.; Gorby, Y.; Kemner, K. M. Characterization of uraninite nanoparticles produced by *Shewanella oneidensis* MR-1. *Geochim. Cosmochim. Acta* **2008**, *72*, 4901−4915.

(8) Bernier-Latmani, R.; Veeramani, H.; Vecchia, E. D.; Junier, P.; Lezama-Pacheco, J. S.; Suvorova, E. I.; Sharp, J. O.; Wigginton, N. S.; Bargar, J. R. Non-uraninite products of microbial U(VI) reduction. *Environ. Sci. Technol.* **2010**, *44*, 9456−9462.

(9) Sharp, J. O.; Lezama-Pacheco, J. S.; Schofield, E. J.; Junier, P.; Ulrich, K.-U.; Chinni, S.; Veeramani, H.; Margot-Roquier, C.; Webb, S. M.; Tebo, B. M.; Giammar, D. E.; Bargar, J. R.; Bernier-Latmani, R. Uranium speciation and stability after reductive immobilization in aquifer sediments. *Geochim. Cosmochim. Acta* **2011**, *75*, 6497−6510.

(10) Loreggian, L.; Sorwat, J.; Byrne, J. M.; Kappler, A.; Bernier-Latmani, R. Role of iron sulfide phases in the stability of noncrystalline tetravalent uranium in sediments. *Environ. Sci. Technol.* **2020**, 4840.

(11) Kelly, S. D.; Kemner, K. M.; Carley, J.; Criddle, C.; Jardine, P. M.; Marsh, T. L.; Phillips, D.; Watson, D.; Wu, W.-M. Speciation of uranium in sediments before and after in situ biostimulation. *Environ. Sci. Technol.* **2008**, *42*, 1558−1564.

(12) Bargar, J. R.; Williams, K. H.; Campbell, K. M.; Long, P. E.; Stubbs, J. E.; Suvorova, E. I.; Lezama-Pacheco, J. S.; Alessi, D. S.; Stylo, M.; Webb, S. M.; Davis, J. A.; Giammar, D. E.; Blue, L. Y.; Bernier-Latmani, R. Uranium redox transition pathways in acetate-amended sediments. *Proc. Natl. Acad. Sci. U. S. A.* **2013**, *110*, 4506−4511.

(13) Stoliker, D. L.; Campbell, K. M.; Fox, P. M.; Singer, D. M.; Kaviani, N.; Carey, M.; Peck, N. E.; Bargar, J. R.; Kent, D. B.; Davis, J. A. Evaluating chemical extraction techniques for the determination of uranium oxidation state in reduced aquifer sediments. *Environ. Sci. Technol.* **2013**, *47*, 9225−9232.

(14) Newsome, L.; Morris, K.; Shaw, S.; Trivedi, D.; Lloyd, J. R. The stability of microbially reduced U(IV); impact of residual electron donor and sediment ageing. *Chem. Geol.* **2015**, *409*, 125−135.

(15) Kelly, S. D.; Wu, W. M.; Yang, F.; Criddle, C. S.; Marsh, T. L.; O'Loughlin, E. J.; Ravel, B.; Watson, D.; Jardine, P. M.; Kemner, K. M. Uranium transformations in static microcosms. *Environ. Sci. Technol.* **2010**, *44*, 236−242.
(16) Finneran, K. T.; Housewright, M. E.; Lovley, D. R. Multiple influences of nitrate on uranium solubility during bioremediation of uranium-contaminated subsurface sediments. *Environ. Microbiol.* **2002**, *4*, 510−516.
(17) Senko, J. M.; Istok, J. D.; Suflita, J. M.; Krumholz, L. R. In-situ evidence for uranium immobilization and remobilization. *Environ. Sci. Technol.* **2002**, *36*, 1491−1496.
(18) Beller, H. R. Anaerobic, nitrate-dependent oxidation of U(IV) oxide minerals by the chemolithoautotrophic bacterium *Thiobacillus denitrificans*. *Appl. Environ. Microbiol.* **2005**, *71*, 2170−2174.
(19) Wan, J.; Tokunaga, T. K.; Brodie, E.; Wang, Z.; Zheng, Z.; Herman, D.; Hazen, T. C.; Firestone, M. K.; Sutton, S. R. Reoxidation of bioreduced uranium under reducing conditions. *Environ. Sci. Technol.* **2005**, *39*, 6162−6169.
(20) Moon, H. S.; Komlos, J.; Jaffé, P. R. Uranium reoxidation in previously bioreduced sediment by dissolved oxygen and nitrate. *Environ. Sci. Technol.* **2007**, *41*, 4587−4592.
(21) Singh, G.; Şengör, S. S.; Bhalla, A.; Kumar, S.; De, J.; Stewart, B.; Spycher, N.; Ginn, T. M.; Peyton, B. M.; Sani, R. K. Reoxidation of biogenic reduced uranium: A challenge toward bioremediation. *Crit. Rev. Environ. Sci. Technol.* **2014**, *44*, 391−415.
(22) Ulrich, K.-U.; Ilton, E. S.; Veeramani, H.; Sharp, J. O.; Bernier-Latmani, R.; Schofield, E. J.; Bargar, J. R.; Giammar, D. E. Comparative dissolution kinetics of biogenic and chemogenic uraninite under oxidizing conditions in the presence of carbonate. *Geochim. Cosmochim. Acta* **2009**, *73*, 6065−6083.
(23) Cerrato, J. M.; Ashner, M. N.; Alessi, D. S.; Lezama-Pacheco, J. S.; Bernier-Latmani, R.; Bargar, J. R.; Giammar, D. E. Relative reactivity of biogenic and chemogenic uraninite and biogenic noncrystalline U(IV). *Environ. Sci. Technol.* **2013**, *47*, 9756−9763.
(24) Riley, R. G.; Zachara, J. M. *Nature of Chemical Contamination on DOE Lands and Identification of Representative Contaminant Mixtures for Basic Subsurface Science Research*; United States DOE, Office of Energy Research: Washington, DC, 1992.
(25) Spain, A. M.; Krumholz, L. R. Nitrate-reducing bacteria at the nitrate and radionuclide contaminated Oak Ridge Integrated Field Research Challenge Site: A review. *Geomicrobiol. J.* **2011**, *28*, 418−429.
(26) Lloyd, J. R.; Renshaw, J. C. Bioremediation of radioactive waste: Radionuclide−microbe interactions in laboratory and field-scale studies. *Curr. Opin. Biotechnol.* **2005**, *16*, 254−260.
(27) Smith, M. B.; Rocha, A. M.; Smillie, C. S.; Olesen, S. W.; Paradis, C.; Wu, L.; Campbell, J. H.; Fortney, J. L.; Mehlhorn, T. L.; Lowe, K. A.; Earles, J. E.; Phillips, J.; Techtmann, S. M.; Joyner, D. C.; Elias, D. A.; Dwayne, A.; Bailey, K. L.; Hurt, R. A.; Preheim, S. P.; Sanders, M. C.; Yang, J.; Mueller, M. A.; Brooks, S.; Watson, D. B.; Zhang, P.; He, Z.; Dubinsky, E. A.; Adams, P. D.; Arkin, A. P.; Fields, M. W.; Zhou, J.; Alm, E. J.; Hazen, T. C. Natural bacterial communities serve as quantitative geochemical biosensors. *MBio* **2015**, *6*, e00326-15.
(28) Van Berk, W.; Fu, Y. Redox roll-front mobilization of geogenic uranium by nitrate input into aquifers: Risks for groundwater resources. *Environ. Sci. Technol.* **2016**, *51*, 337−345.
(29) Banning, A.; Demmel, T.; Rüde, T. R.; Wrobel, M. Groundwater uranium origin and fate control in a river valley aquifer. *Environ. Sci. Technol.* **2013**, *47*, 13941−13948.
(30) Nolan, J.; Weber, K. A. Natural uranium contamination in major U.S. aquifers linked to nitrate. *Environ. Sci. Technol. Lett.* **2015**, *2*, 215−220.
(31) Senko, J. M.; Mohamed, Y.; Dewers, T. A.; Krumholz, L. R. Role for Fe(III) minerals in nitrate-dependent microbial U(IV) oxidation. *Environ. Sci. Technol.* **2005**, *39*, 2529−2536.
(32) Beller, H. R.; Chain, P. S. G.; Letain, T. E.; Chakicherla, A.; Larimer, F. W.; Richardson, P. M.; Coleman, M. A.; Wood, A. P.; Kelly, D. P. The genome sequence of the obligately chemolithoautotrophic, facultatively anaerobic bacterium *Thiobacillus denitrificans*. *J. Bacteriol.* **2006**, *188*, 1473−1488.
(33) Straub, K. L.; Benz, M.; Schink, B.; Widdel, F. Anaerobic, nitrate-dependent microbial oxidation of ferrous iron. *Appl. Environ. Microbiol.* **1996**, *62*, 1458−1460.
(34) Torrentó, C.; Cama, J.; Urmeneta, J.; Otero, N.; Soler, A. Denitrification of groundwater with pyrite and *Thiobacillus denitrificans*. *Chem. Geol.* **2010**, *278*, 80−91.
(35) Beller, H. R.; Zhou, P.; Legler, T. C.; Chakicherla, A.; Kane, S.; Letain, T. E.; O'Day, P. A. Genome-enabled studies of anaerobic, nitrate-dependent iron oxidation in the chemolithoautotrophic bacterium *Thiobacillus denitrificans*. *Front. Microbiol.* **2013**, *4*, 249.
(36) Beller, H. R.; Letain, T. E.; Chakicherla, A.; Kane, S. R.; Legler, T. C.; Coleman, M. A. Whole-genome transcriptional analysis of chemolithoautotrophic thiosulfate oxidation by *Thiobacillus denitrificans* under aerobic versus denitrifying conditions. *J. Bacteriol.* **2006**, *188*, 7005−7015.
(37) Wu, W.-M.; Carley, J.; Green, S. J.; Luo, J.; Kelly, S. D.; van Nostrand, J.; Lowe, K.; Mehlhorn, T.; Carroll, S.; Boonchayanant, B.; Löffler, F. E.; Watson, D.; Kemner, K. M.; Zhou, J.; Kitanidis, P. K.; Kostka, J. E.; Jardine, P. M.; Criddle, C. S. Effects of nitrate on the stability of uranium in a bioreduced region of the subsurface. *Environ. Sci. Technol.* **2010**, *44*, 5104−5111.
(38) Beller, H. R.; Legler, T. C.; Bourguet, F.; Letain, T. E.; Kane, S. R.; Coleman, M. A. Identification of *c*-type cytochromes involved in anaerobic, bacterial U(IV) oxidation. *Biodegradation* **2009**, *20*, 45−53.
(39) Bruno, J.; Casas, I.; Puigdomènech, I. The kinetics of dissolution of UO_2 under reducing conditions and the influence of an oxidized surface layer (UO_{2+x}): Application of a continuous flow-through reactor. *Geochim. Cosmochim. Acta* **1991**, *55*, 647−658.
(40) Giménez, J.; Clarens, F.; Casas, I.; Rovira, M.; de Pablo, J.; Bruno, J. Oxidation and dissolution of UO_2 in bicarbonate media: Implications for the spent nuclear fuel oxidative dissolution mechanism. *J. Nucl. Mater.* **2005**, *345*, 232−238.
(41) Ulrich, K.-U.; Singh, A.; Schofield, E. J.; Bargar, J. R.; Veeramani, H.; Sharp, J. O.; Bernier-Latmani, R.; Giammar, D. E. Dissolution of biogenic and synthetic UO_2 under varied reducing conditions. *Environ. Sci. Technol.* **2008**, *42*, 5600−5606.
(42) Frazier, S. W.; Kretzschmar, R.; Kraemer, S. M. Bacterial siderophores promote dissolution of UO_2 under reducing conditions. *Environ. Sci. Technol.* **2005**, *39*, 5709−5715.
(43) Handley-Sidhu, S.; Bryan, N. D.; Worsfold, P. J.; Vaughan, D. J.; Livens, F. R.; Keith-Roach, M. J. Corrosion and transport of depleted uranium in sand-rich environments. *Chemosphere* **2009**, *77*, 1434−1439.
(44) Veeramani, H.; Schofield, E. J.; Sharp, J. O.; Suvorova, E. I.; Ulrich, K.-U.; Mehta, A.; Giammar, D. E.; Bargar, J. R.; Bernier-Latmani, R. Effect of Mn(II) on the structure and reactivity of biogenic uraninite. *Environ. Sci. Technol.* **2009**, *43*, 6541−6547.
(45) Bi, Y.; Stylo, M.; Bernier-Latmani, R.; Hayes, K. F. Rapid mobilization of noncrystalline U(IV) coupled with FeS oxidation. *Environ. Sci. Technol.* **2016**, *50*, 1403−1411.
(46) Fredrickson, J. K.; Zachara, J. M.; Kennedy, D. W.; Duff, M. C.; Gorby, Y. A.; Li, S. M. W.; Krupka, K. M. Reduction of U(VI) in goethite (α-FeOOH) suspensions by a dissimilatory metal-reducing bacterium. *Geochim. Cosmochim. Acta* **2000**, *64*, 3085−3098.
(47) Pierce, E. M.; Icenhower, J. P.; Serne, R. J.; Catalano, J. G. Experimental determination of UO_2(Cr) dissolution kinetics: Effects of solution saturation state and pH. *J. Nucl. Mater.* **2005**, *345*, 206−218.
(48) Allen, P. G.; Shuh, D. K.; Bucher, J. J.; Edelstein, N. M.; Palmer, C. E. A.; Silva, R. J.; Nguyen, S. N.; Marquez, L. N.; Hudson, E. A. Determination of uranium structures by EXAFS: Schoepite and other U(VI) oxide precipitates. *Radiochim. Acta* **1996**, *75*, 47−53.
(49) Chakraborty, S.; Favre, F.; Banerjee, D.; Scheinost, A. C.; Mullet, M.; Ehrhardt, J.-J.; Brendle, J.; Vidal, L.; Charlet, L. U(VI) Sorption and reduction by Fe(II) sorbed on montmorillonite. *Environ. Sci. Technol.* **2010**, *44*, 3779−3785.

https://dx.doi.org/10.1021/acs.est.0c01019
Environ. Sci. Technol. 2020, 54, 8010−8021

(50) Alessi, D. S.; Uster, B.; Veeramani, H.; Suvorova, E. I.; Lezama-Pacheco, J. S.; Stubbs, J. E.; Bargar, J. R.; Bernier-Latmani, R. Quantitative separation of monomeric U(IV) from UO_2 in products of U(VI) reduction. *Environ. Sci. Technol.* **2012**, *46*, 6150−6157.
(51) Boyanov, M. I.; Fletcher, K. E.; Kwon, M. J.; Rui, X.; O'Loughlin, E. J.; Löffler, F. E.; Kemner, K. M. Solution and microbial controls on the formation of reduced U(IV) species. *Environ. Sci. Technol.* **2011**, *45*, 8336−8344.
(52) Morin, G.; Mangeret, A.; Othmane, G.; Stetten, L.; Seder-Colomina, M.; Brest, J.; Ona-Nguema, G.; Bassot, S.; Courbet, C.; Guillevic, J.; Thouvenot, A.; Mathon, O.; Proux, O.; Bargar, J. R. Mononuclear U(IV) complexes and ningyoite as major uranium species in lake sediments. *Geochemical Perspect. Lett.* **2016**, 95−105.
(53) Stetten, L.; Mangeret, A.; Brest, J.; Seder-Colomina, M.; Le Pape, P.; Ikogou, M.; Zeyen, N.; Thouvenot, A.; Julien, A.; Alcalde, G.; Reyss, J. L.; Bombled, B.; Rabouille, C.; Olivi, L.; Proux, O.; Cazala, C.; Morin, G. Geochemical control on the reduction of U(VI) to mononuclear U(IV) species in lacustrine sediments. *Geochim. Cosmochim. Acta* **2018**, *222*, 171−186.
(54) Stetten, L.; Blanchart, P.; Mangeret, A.; Lefebvre, P.; Le Pape, P.; Brest, J.; Merrot, P.; Julien, A.; Proux, O.; Webb, S. M.; Bargar, J. R.; Cazala, C.; Morin, G. Redox fluctuations and organic complexation govern uranium redistribution from U(IV)-phosphate minerals in a mining-polluted wetland soil, Brittany, France. *Environ. Sci. Technol.* **2018**, *52*, 13099−13109.
(55) Mikutta, C.; Langner, P.; Bargar, J. R.; Kretzschmar, R. Tetra- and hexavalent Uranium forms bidentate-mononuclear complexes with particulate organic matter in a naturally uranium-enriched peatland. *Environ. Sci. Technol.* **2016**, *50*, 10465−10475.
(56) Shoesmith, D. W. Fuel corrosion processes under waste disposal conditions. *J. Nucl. Mater.* **2000**, *282*, 1−31.
(57) Santos, B. G.; Nesbitt, H. W.; Noël, J. J.; Shoesmith, D. W. X-ray photoelectron spectroscopy study of anodically oxidized SIMFUEL surfaces. *Electrochim. Acta* **2004**, *49*, 1863−1873.
(58) Santos, B. G.; Noël, J. J.; Shoesmith, D. W. The effect of pH on the anodic dissolution of SIMFUEL (UO_2). *J. Electroanal. Chem.* **2006**, *586*, 1−11.
(59) Christensen, H.; Sunder, S.; Shoesmith, D. W. Oxidation of Nuclear Fuel (UO_2) by the products of water radiolysis: Development of a kinetic model. *J. Alloys Compd.* **1994**, *213*−*214*, 93−99.
(60) Hatakeyama, K.; Park, Y.-Y.; Tomiyasu, H.; Wada, Y.; Ikeda, Y. Photo-enhancement effect on oxidation reaction of Uranium(IV) by NO_3^- in perchloric acid solutions. *J. Nucl. Sci. Technol.* **1997**, *34*, 695−699.
(61) Giammar, D. E.; Cerrato, J. M.; Mehta, V.; Wang, Z.; Wang, Y.; Pepping, T. J.; Ulrich, K.-U.; Lezama-Pacheco, J. S.; Bargar, J. R. Effect of diffusive transport limitations on UO_2 dissolution. *Water Res.* **2012**, *46*, 6023−6032.
(62) Reinoso-Maset, E.; Steefel, C. I.; Um, W.; Chorover, J.; O'Day, P. A. Rates and mechanisms of uranyl oxyhydroxide mineral dissolution. *Geochim. Cosmochim. Acta* **2017**, *207*, 298−321.
(63) Pérez, I.; Casas, I.; Martín, M.; Bruno, J. The thermodynamics and kinetics of uranophane dissolution in bicarbonate test solutions. *Geochim. Cosmochim. Acta* **2000**, *64*, 603−608.
(64) Ilton, E. S.; Liu, C.; Yantasee, W.; Wang, Z.; Moore, D. A.; Felmy, A. R.; Zachara, J. M. The dissolution of synthetic Na-Boltwoodite in sodium carbonate solutions. *Geochim. Cosmochim. Acta* **2006**, *70*, 4836−4849.
(65) Gudavalli, R. K. P.; Katsenovich, Y. P.; Wellman, D. M.; Idarraga, M.; Lagos, L. E.; Tansel, B. Comparison of the kinetic rate law parameters for the dissolution of natural and synthetic autunite in the presence of aqueous bicarbonate ions. *Chem. Geol.* **2013**, *351*, 299−309.
(66) Spycher, N. F.; Issarangkun, M.; Stewart, B. D.; Sevinç Şengör, S.; Belding, E.; Ginn, T. R.; Peyton, B. M.; Sani, R. K. Biogenic uraninite precipitation and its reoxidation by Iron(III) (Hydr)Oxides: A reaction modeling approach. *Geochim. Cosmochim. Acta* **2011**, *75*, 4426−4440.
(67) Newsome, L.; Morris, K.; Lloyd, J. R. The Biogeochemistry and Bioremediation of uranium and other priority radionuclides. *Chem. Geol.* **2014**, *363*, 164−184.
(68) Casas, I.; Giménez, J.; Marti, V.; Torrero, M. E.; De Pablo, J. Kinetic studies of unirradiated UO_2 dissolution under oxidizing conditions in batch and flow experiments. *Radiochim. Acta* **1994**, *66*−*67*, 23−27.
(69) Bruno, J.; Casas, I.; Cera, E.; De Pablo, J.; GimÉnez, J.; Torrero, M. E. Uranium (IV) dioxide and SIMFUEL as chemical analogues of nuclear spent fuel matrix dissolution. A comparison of dissolution results in a standard $NaCl/NaHCO_3$ solution. *Sci. Basis Nucl. Waste Manag. XVII.* 1995, *Symposium,* 601−608.
(70) Mailloux, B. J.; Kim, C.; Kichuk, T.; Nguyen, K.; Precht, C.; Wang, S.; Jewell, T. N. M.; Karaoz, U.; Brodie, E. L.; Williams, K. H.; Beller, H. R.; Buchholz, B. A. Paired RNA radiocarbon and sequencing analyses indicate the importance of autotrophy in a shallow alluvial aquifer. *Sci. Rep.* **2019**, *9*, 10370.
(71) Cardenas, E.; Wu, W. M.; Leigh, M. B.; Carley, J.; Carroll, S.; Gentry, T.; Luo, J.; Watson, D.; Gu, B.; Ginder-Vogel, M.; Kitanidis, P. K.; Jardine, P. M.; Zhou, J.; Criddle, C. S.; Marsh, T. L.; Tiedje, J. M. Microbial communities in contaminated sediments, associated with bioremediation of uranium to submicromolar levels. *Appl. Environ. Microbiol.* **2008**, *74*, 3718−3729.

https://dx.doi.org/10.1021/acs.est.0c01019
Environ. Sci. Technol. 2020, 54, 8010−8021